

# New Electrochemical Characterization Methods for Nanocomposite Supercapacitor Electrodes

Jason Ma

*Department of Physics and Astronomy, University of California, Los Angeles, CA 90024*

Supercapacitor electrodes fabricated from a nanocomposite consisting of multiwall carbon nanotubes and titanium oxide nanoparticles were characterized electrochemically. Conventional electrochemical characterizations cyclic voltammetry and galvanostatic charge-discharge in a lithium-based electrolyte gave a specific capacitance of 345 F/g at a current density of 0.1 A/g. New electrochemical characterization techniques that allow one to obtain the peak capacitance associated with intercalation and to distinguish between electrostatic and faradaic charge storage are described and applied to the electrode measurements. Finally, the maximum energy density obtained was 31 Wh/kg.

## I. Introduction

Supercapacitors, also called ultracapacitors or electrochemical double layer capacitors (EDLCs), bridge the gap between batteries and conventional dielectric capacitors [1, 2]. The most common electrode material is carbon-based and include activated carbon [1, 3, 4], carbon nanotubes [5–11], and graphene [12, 13]. To go beyond electrostatic charge storage in the double layer, pseudocapacitive and faradaic components (faradaic components henceforth) such as conducting polymers and metal oxides were incorporated into supercapacitors [3, 14–16]. Two ways of incorporating the faradaic material have been employed, both in an asymmetric (or hybrid) configuration where: (1) a carbon electrode and a faradaic electrode form the two electrodes of a supercapacitor [17–21]; (2) at least one of the electrodes is a composite material that combines advantages of electrochemical double layer charge storage as well as surface redox or intercalation charge storage [22–26].

Carbon nanotubes (CNT) have a high aspect ratio and form porous networks with good conductivity. As such, they have been implemented as supercapacitor electrodes in many instances in the literature [1, 3, 5, 7–11, 27, 28]. Titanium oxide is a versatile compound and can be found in several energy harvesting and energy storage applications, namely photocatalysis, secondary batteries, and supercapacitors [29]. Among the three polymorphs of  $\text{TiO}_2$ , the crystal structure of anatase can accommodate the most  $\text{Li}^+$  per  $\text{TiO}_2$  unit and is an attractive energy storage material due to its  $\text{Li}$ -intercalation capabilities and cycle life [30].  $\text{TiO}_2$  nanowires have been synthesized by hydrothermal methods, functioning as the anode of a supercapacitor with carbon nanotubes acting as the cathode [19, 20]. These are type (1) asymmetric supercapacitors.

In this study, the application of a nanocomposite containing  $\text{TiO}_2$  nanoparticles and multiwall carbon nanotubes in a single supercapacitor electrode is reported. Results from conventional as well as new electrochemical characterization methods show not only the various aspects of the energy storage mechanism in the electrode but also the combination of double layer and faradaic capacitance as a synergy that leads to high energy density and good power density in a single electrode.

## II. Experimental Section

### A. Conventional Electrochemical Characterization

Cyclic voltammetry (CV) as well as galvanostatic cycling (GC) were performed on the CNT- $\text{TiO}_2$  composite electrodes. Cyclic voltammetry of the composite electrode at various scan rates was measured in 1 M  $\text{LiClO}_4$  in propylene carbonate with lithium metal sheets as the reference electrode and counter electrode, shown in Figure 1. The voltage window was 1 V to 2.6 V vs.  $\text{Li}/\text{Li}^+$ . A series of galvanostatic measurements were also performed, two of which are shown in Figure 2.

The electrode capacitance is given by  $C = Q/\Delta V$  and the specific capacitance by  $C_{sp} = C/M$ . The storage capacity of the composite electrode decreases with increasing current but approaches a constant value, shown in Figure 3 along with the coulombic efficiency.

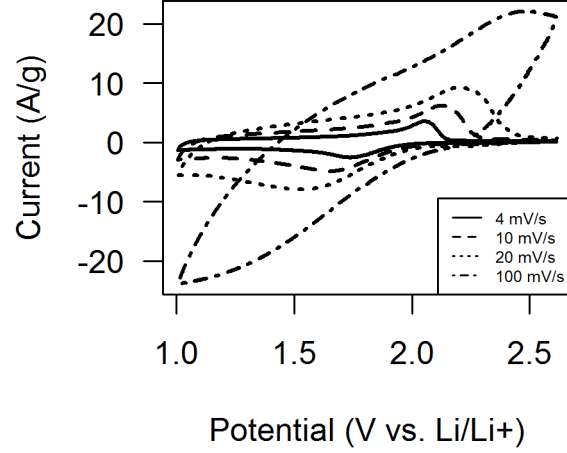


FIG. 1: Cyclic voltammograms (CVs) of CNT-TiO<sub>2</sub> composite electrode at various scan rates in 1 M LiClO<sub>4</sub> in propylene carbonate with lithium metal sheets as the reference electrode and counter electrode.

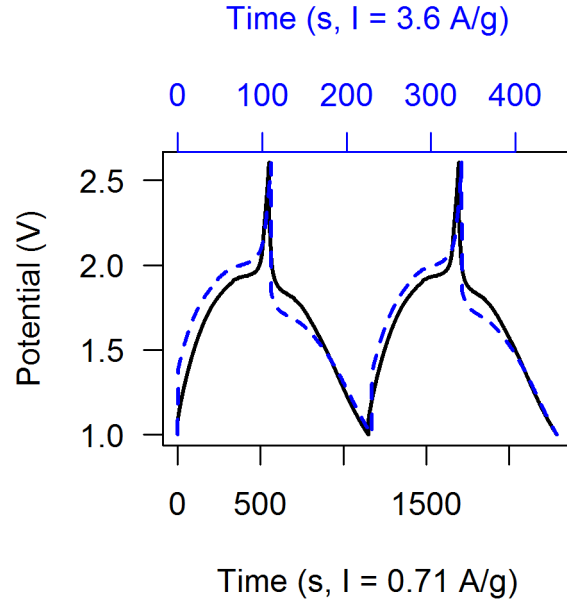


FIG. 2: Galvanostatic measurements of CNT-TiO<sub>2</sub> composite electrode with applied currents densities 0.71 A/g and 3.6 A/g.

### B. New Electrochemical Characterization Methods

The galvanostatic charging for a given current  $I$  is described by

$$V = \frac{I}{C}t + IR_s \quad (1)$$

where  $C$  is the capacitance of the electrode and  $R_s$  is the internal resistance. The quantity  $IR_s$ , denoted by  $V_d$ , is the voltage drop at the beginning of charging and discharging cycles. The temporal slope  $dt/dV$  plotted as a function of

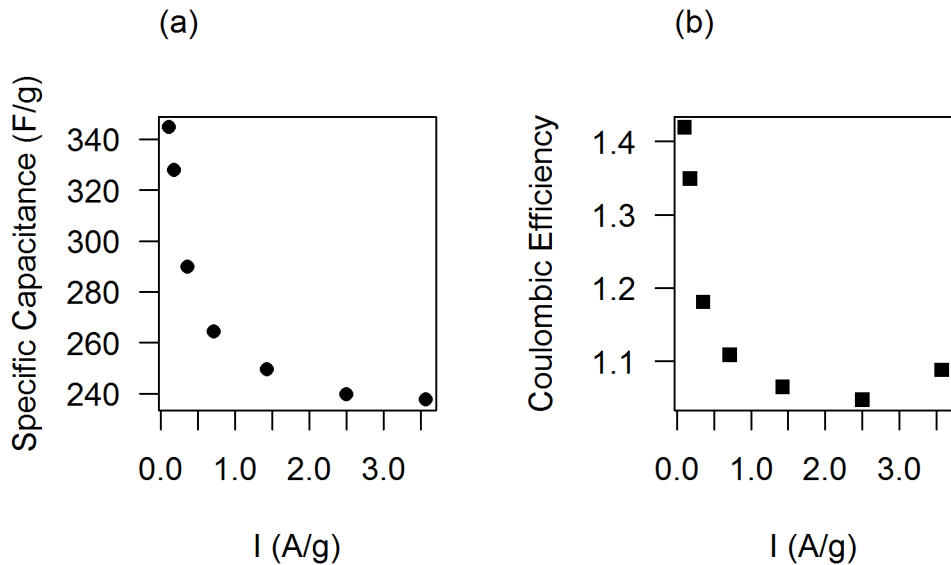


FIG. 3: (a) Specific capacitance vs. current density. (b) Coulombic efficiency.

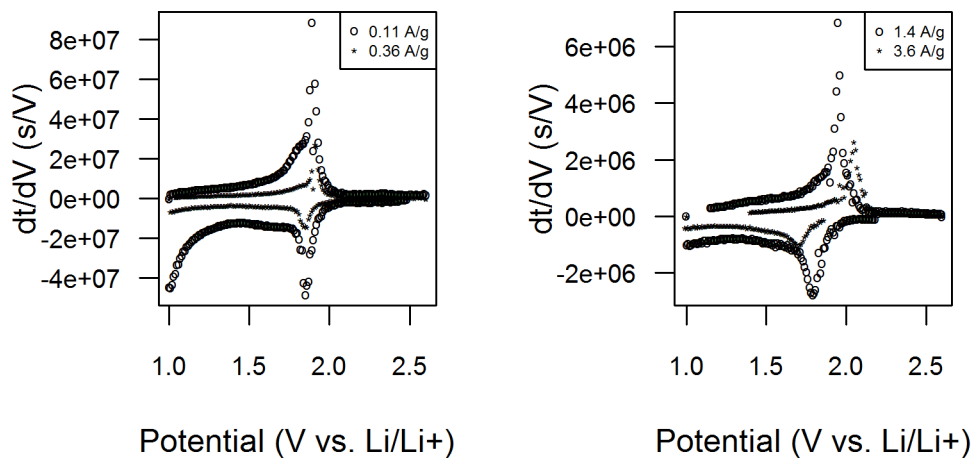


FIG. 4: Temporal slope voltammograms were constructed from galvanostatic measurements at current densities 0.11, 0.36, 1.4, and 3.6 A/g.

the potential is shown in Figure 4. These plots will be called temporal slope voltammograms (TSVs) in this article. Similar to CVs, the anodic peaks and cathodic peaks shift as the applied current increases. However, whereas the faradaic/intercalation peaks flatten as the scan rates increase in CVs, the temporal slope peaks remain sharp even for large current densities.

As shown in Figure 5a, as  $V_d$  vanishes, both anodic and cathodic peak potentials approach the same value, the standard potential for the intercalation reaction. A plot of the temporal slope peaks versus  $I^{-1}$  shows a linear relationship (Figure 5b). Linear regression gives the peak capacitances at  $V_p$ , 2410 F/g for Li extraction and 1450 F/g for Li insertion. As a point of reference, the theoretical specific capacitance of  $\text{TiO}_2$  assuming one  $\text{Li}^+$  ion per  $\text{TiO}_2$

molecule is 2295 F/g, calculated using the formula  $FV_p/\rho_{TiO_2}$ , where  $F$  is the faraday constant and  $\rho_{TiO_2}$  is the  $TiO_2$  molar mass. The peak capacitance at the standard potential of the faradaic reaction could be an important figure of merit in characterizing and optimizing nanocomposites as the mass normalized quantity is nearly independent of the double layer contributions.

In addition to temporal slope voltammograms, a new method to distinguish between electrostatic and faradaic contributions to the energy storage capacity warrants discussion. The distinction is important because one is often interested in the effect of nanoparticle size on the faradaic reactions and whether the faradaic process involves only surface sites or the bulk [31]. The differential form of the capacitor equation

$$dq = CdV + VdC \quad (2)$$

includes both capacitor behavior, where the capacitance is a constant that depends only on the capacitor's geometry and dielectric material, and battery behavior, where the potential is ideally constant and the storage capacity varies linearly with the state of charge. In the case where the potential is the experimentally tunable parameter, charge conservation requires

$$\frac{dq}{dV} = C + V\frac{dC}{dV} \quad (3)$$

The current associated with changes in the double layer is given by  $I_{dl} = C_{dl}dV/dt$  and the current due to reversible charge transfer reactions at the electrode surface is described by [32]

$$I_F = \frac{(nF)^2}{RT} \delta AC_O^o \frac{e^{\mathcal{F}(V^o - V)}}{(1 + e^{\mathcal{F}(V^o - V)})^2} \frac{dV}{dt} \quad (4)$$

where  $\mathcal{F} = nF/RT$ ,  $C_O^o$  is the starting and ion concentration at the electrode-electrolyte interface,  $\delta$  is the width of the diffusion layer,  $A$  is the area of the  $TiO_2$  nanoparticles, and  $V^o$  is the standard potential of the reaction. It follows that the charge stored is

$$q(V) = nF\delta AC_O^o \left( \frac{1}{1 + e^{\mathcal{F}(V^o - V)}} - \frac{1}{1 + e^{\mathcal{F}V^o}} \right) + C_{dl}V \quad (5)$$

The charge accumulation as a function of potential can be obtained from galvanostatic measurements, as shown in Figure 6. The double layer capacitance can be obtained from the slope of  $q(V)$  for sufficiently large potentials, after available  $TiO_2$  lattice sites are fully intercalated.

### III. Results and Discussion

Dielectric capacitors experience changes in potential at a constant storage capacity, whereas batteries experience changes in the storage capacity at a constant potential. The methods outlined in this article enable researchers to electrochemically characterize nanocomposites that exhibit both capacitor-like and battery-like behaviors.

The performance of the CNT- $TiO_2$  electrode can be compared to lithium-ion batteries and other electrochemical capacitors in the form of a ragone chart, shown in Figure 7. The storage capacity and the voltage range can be converted to energy density and power density with the formulas

$$ED = \frac{1}{8} \frac{C_{sp}\Delta V^2}{3.6}, \quad PD = \frac{\Delta V^2}{8MR_s}$$

The synergy between the two materials gives rise to high energy and good power. From the perspective of the high energy density Li-intercalation material, namely the  $TiO_2$  nanoparticles, the addition of carbon nanotubes led to a significant increase in power density.

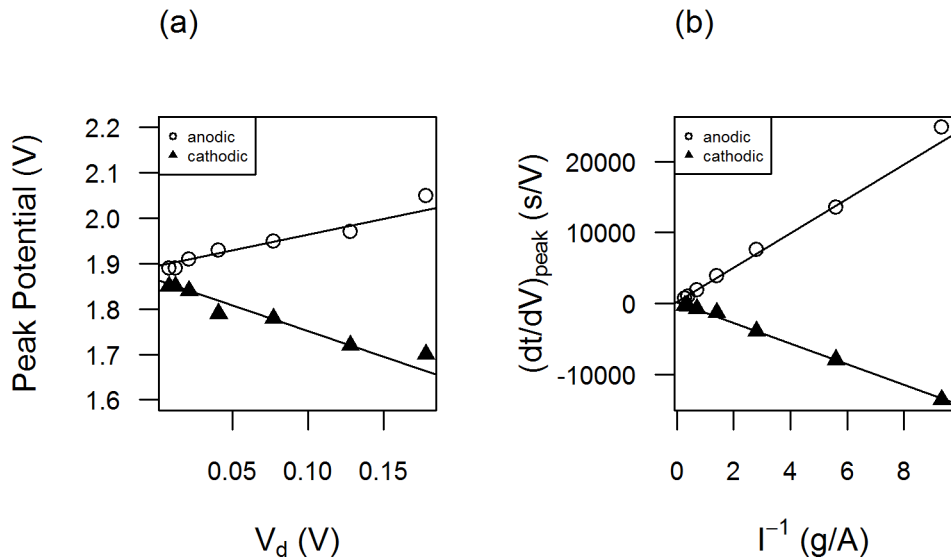


FIG. 5: (a) The peak potential is linear in the voltage drop  $V_d$ . The anodic and cathodic intercepts are both 1.9 V. (b) Temporal slope peaks are linear in  $I^{-1}$ . The absolute values of the two linear regression slopes yield peak capacitances.

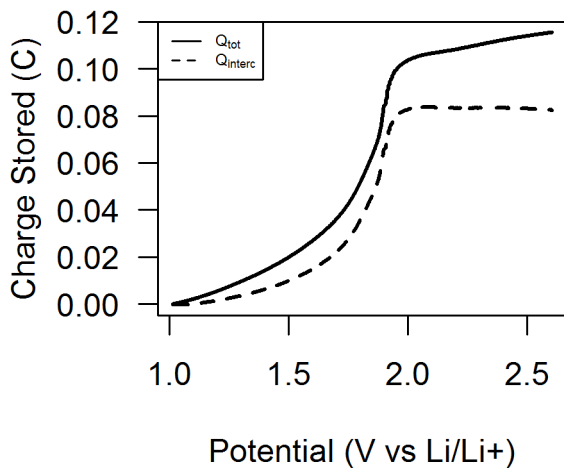


FIG. 6: Charge accumulated as a function of potential for a current density of 0.1 A/g.

#### IV. Conclusion

A supercapacitor electrode was fabricated from a nanocomposite consisting of multiwall carbon nanotubes and titanium oxide nanoparticles. Conventional electrochemical characterizations cyclic voltammetry and galvanostatic cycling gave a specific capacitance of 345 F/g at a current density of 0.1 A/g. New electrochemical characterization techniques derived from galvanostatic measurements allow one to obtain the peak capacitance associated with intercalation and to distinguish between electrostatic and faradaic contributions to the total charge stored. The new techniques show that most of the charge is stored faradaically, via the intercalation mechanism. The double

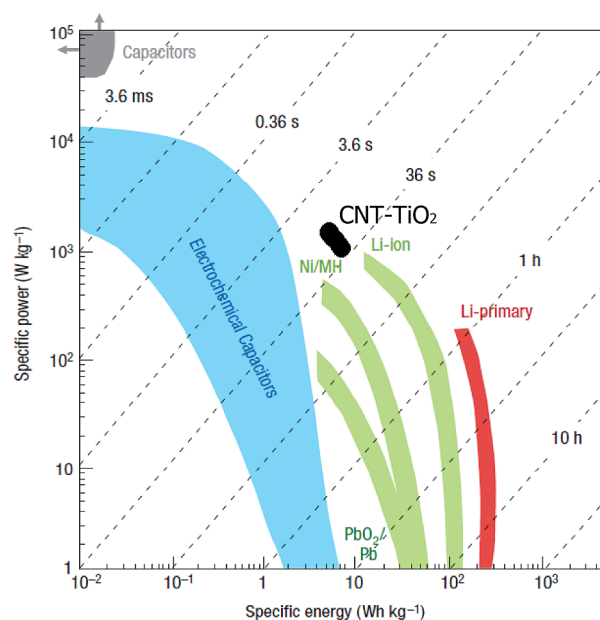


FIG. 7: Ragone chart showing the performance of the CNT-TiO<sub>2</sub> electrode with respect to Li-ion batteries and other electrochemical capacitors. [Adapted from Ref. 18 with permission.]

layer charge storage mainly attributed to carbon nanotubes brought significant improvement in power density to the faradaic material. As a nanocomposite, CNT-TiO<sub>2</sub> achieved a maximum energy density of 31 Wh/kg.

### Acknowledgement

Helpful discussions from George Grüner, Bruce Dunn, Ryan Maloney, Veronica Augustyn as well as measurement support and TiO<sub>2</sub> nanoparticles from Veronica and Jesse Ko are acknowledged and appreciated.

- 
- [1] A.G. Pandolfo and A.F. Hollenkamp. *J. Power Sources*, 157:11, 2006.
  - [2] G.A. Snook, P. Kao and A.S. Best. *J. Power Sources*, 196:1, 2011.
  - [3] E. Frackowiak and F. Béguin. *Carbon*, 39:937, 2001.
  - [4] L.L. Zhang and X.S. Zhao. *Chem. Soc. Rev.*, 38:2520, 2009.
  - [5] G. Grüner, G. Wee, M. Kaempgen, J. Ma and S.G. Mhaisalkar. *Appl. Phys. Lett.*, 90:264104, 2007.
  - [6] F. Wudl, I. Weitz, C. Liu, A.J. Bard and J.R. Heath. *Electrochem. Solid-State Lett.*, 2:577, 1999.
  - [7] J. Yeh, C. Du and N. Pan. *Nanotechnology*, 16:350, 2005.
  - [8] M. Kaempgen, C.K. Chan, J. Ma, Y. Cui and G. Grüner. *Nano Letters*, 9:1872, 2009.
  - [9] V. Bertagna, E. Frackowiak, K. Metenier and F. Béguin. *Appl. Phys. Lett.*, 77:2421, 2000.
  - [10] S. Delpoux V. Bertagna S. Bonnamy Frackowiak, K. Jurewicz and F. Béguin. Aip conference proceedings. volume 544, pages 533–536. AIP Publishing, 2000.
  - [11] M. Meyyappan. *J. Vac. Sci. Technol. A*, 31:050803, 2013.
  - [12] S. Biswas and L.T. Drzal. *Chemistry of Materials*, 22:5667, 2010.
  - [13] Y. Huang, Y. Ma, C. Wang, M. Chen, Y. Wang, Z. Shi and Y. Chen. *J. Phys. Chem. C*, 113:13103, 2009.
  - [14] M.R. Watt, R.A. Fisher and W.J. Ready. *ECS J. Solid State Sci. Technol.*, 2:M3170, 2013.
  - [15] B.E. Conway and W.G. Pell. *J. Solid State Electrochem.*, 7:637, 2003.
  - [16] D. Cericola and R. Ktz. *Electrochim. Acta*, 72:1, 2012.
  - [17] J.P. Zheng. *J. Electrochem. Soc.*, 150:A484, 2003.
  - [18] P. Simon and Y. Gogotsi. *Nat. Mater.*, 7:845, 2008.
  - [19] Z.H. Wen, Q. Wang and J.H. Li. *Adv. Funct. Mater.*, 16:2141, 2006.
  - [20] J.N. Wu, G. Wang, Z.Y. Liu and Q. Lu. *Mater. Lett.*, 71:120, 2012.
  - [21] M.-L. Zhang, Y. Xue, Y. Chen and Y.-D. Yan. *Mater. Lett.*, 62:3884, 2008.

- [22] E. Frackowiak, V. Khomenko, E. Raymundo-Piero and F. Béguin. *Appl. Phys. A*, 82:567, 2006.
- [23] D. Weng, Q. Xiao, Y. Peng, X. Wang, H. Li, F. Wei Z. Chen, Y. Qin and Y. Lu. *Adv. Funct. Mater.*, 19:3420, 2009.
- [24] T. Wang, A. Kiebele, J. Ma, S. Mhaisalkar and G. Grüner. *J. Electrochem. Soc.*, 158:A1, 2011.
- [25] X.S. Zhao K. Zhang, L.L. Zhang and J. Wu. *Chem. Mater.*, 22:1392, 2010.
- [26] B. Shao, Z. Fan, W. Qian, M. Zhang, J. Yan, T. Wei and F. Wei. *Carbon*, 48:487, 2010.
- [27] R. Hoch, D. Moy, C. Niu, E.K. Sichel and H. Tennent. *Appl. Phys. Lett.*, 70:1480, 1997.
- [28] Y.S. Park, Y.C. Choi, S.M. Lee, D.C. Chung, D.J. Bae, S.C. Lim K.H. An, W.S. Kim and Y.H. Lee. *Adv. Mater.*, 13:497, 2001.
- [29] J.M. Friedrich, D.V. Bavykin and F.C. Walsh. *Adv. Mater.*, 18:2807, 2006.
- [30] S. Kerisit, K.M. Rosso D. Wang, J. Zhang, G. Graff, Z. Yang, D. Choi and J. Liu. *J. Power Sources*, 192:588, 2009.
- [31] J. Lim, J. Wang, J. Polleux and B. Dunn. *J. Phys. Chem. C*, 111:14925, 2007.
- [32] A.J. Bard and L.R. Faulkner. *Electrochemical Methods: Fundamentals and Applications*. Wiley, 2000.